Translocation of β-Galactosidase Mediated by the Cell-Penetrating Peptide Pep-1 into Lipid Vesicles and Human HeLa Cells Is Driven by Membrane Electrostatic Potential†

Sónia Troeira Henriques,‡ Júlia Costa,§ and Miguel A. R. B. Castanho*,‡

Centro de Química e Bioquímica, Faculdade de Ciências da Universidade de Lisboa, Ed. C8, Campo Grande, 1749-016 Lisboa, Portugal, and Instituto de Tecnologia Química e Biológica, Apartado 127, 2780 Oeiras, Portugal

Received February 14, 2005; Revised Manuscript Received May 25, 2005

ABSTRACT: The cell-penetrating peptide (CPP) pep-1 is capable of introducing large proteins into different cell lines, maintaining their biological activity. Two possible mechanisms have been proposed to explain the entrance of other CPPs in cells, endosomal-dependent and independent types. In this work, we evaluated the molecular mechanisms of pep-1-mediated cellular uptake of β-galactosidase (β-Gal) from *Escherichia coli* in large unilamellar vesicles (LUV) and HeLa cells. Fluorescence spectroscopy was used to evaluate the translocation process in model systems (LUV). Immunofluorescence microscopy was used to study the translocation in HeLa cells. Enzymatic activity detection enabled us to monitor the internalization of β-Gal into LUV and the functionality of the protein in the interior of HeLa cells. β-Gal translocated into LUV in a transmembrane potential-dependent manner. Likewise, the extent of β-Gal incorporation was extensively decreased in depolarized cells. Furthermore, β-Gal uptake efficiency and kinetics were temperature-independent, and β-Gal did not colocalize with endosomes, lysosomes, or caveosomes. Therefore, β-Gal translocation was not associated with the endosomal pathway. Although an excess of pep-1 was mandatory for β-Gal translocation in vivo, transmembrane pores were not formed as concluded from the trypan blue exclusion method. These results altogether indicated that protein uptake both in vitro with LUV and in vivo with HeLa cells was mainly, if not solely, dependent on negative transmembrane potential across the bilayer, which suggests a physical mechanism governed by electrostatic interactions between pep-1 (positively charged) and membranes (negatively charged).

The introduction of hydrophilic molecules into mammalian cells has become a key strategy for the investigation of intracellular processes and drug therapy. CPPs[1] are very attractive for these purposes because of their ability to mediate cellular uptake of proteins and nucleic acids, which is otherwise impossible because of membrane selective permeability (*1*−*7*). These peptides are small (9−33 amino acid residues), and their only common feature is the presence of basic amino acid residues (*2*).

The most widely used CPPs are derived from HIV-1 tat (TAT) and *Drosophila* Antennapedia homoprotein (*1*, *4*, *6*). Covalent linkage of CPP with cargo molecules leads to their nontoxic import into cells, both rapidly and efficiently, while maintaining functional activity inside the cell (*2*). The process, however, is dependent on CPP, cargo, and cell type (*8*). The translocation of these cationic peptides is not well understood. A single general mechanism for all does not seem reasonable, and there are examples of CPPs (e.g., TAT) that are able to use both endosomal and nonendosomal pathways (*5*, *9*).

Pep-1 (Ac-KETWWETWWTEWSQPKKKRKV-cysteamine) is an artificial CPP that has the ability to establish hydrophobic interactions with the cargo molecule, which may render covalent links unnecessary and favor the native structure (*10*). This sequence contains a Trp-rich hydrophobic domain, KETWWETWWTEW, a hydrophilic sequence, KKKRKV, that is the nuclear localization sequence of simian virus 40 large T antigen, and a spacer, SQP, linking the two previous ones (*10*). This peptide has been successfully used to translocate different biomolecules into distinct cell lines, for instance, proteins into protoplasts (*11*), antibodies into

† This work was funded by Grant POCTI/BCI/38631 from FCT, Portugal, and Grant LSHG-CT-2004-503228 from the European Commission. We thank FCT, Portugal, for Grant SFRH/BD/14337/2003 under the program POCTI to S.T.H.

* To whom correspondence should be addressed. Telephone: +351217500931. Fax: +351217500088. E-mail: castanho@fc.ul.pt.

‡ Faculdade de Ciências da Universidade de Lisboa.

§ Instituto de Tecnologia Química e Biológica.

[1] Abbreviations: CPP, cell-penetrating peptide; NLS, nuclear localization sequence; SV-40, simian virus 40; TAT, CPP derived from HIV-1 tat; β-Gal, β-galactosidase; LUV, large unilamellar vesicles; MUG, 4-methylumbelliferyl galactoside; 4-MU, 4-methylumbelliferone; PMSF, phenylmethanesulfonyl fluoride; phosphine, tris(2-cyanoethyl)-phosphine; POPC, 1-palmitoyl-2-oleoyl-*sn*-glycero-3-phosphocholine; POPG, 1-palmitoyl-2-oleoyl-*sn*-glycero-3-[phospho-*rac*-(1-glycerol)]; DPPC, 1,2-dipalmitoyl-*sn*-glycero-3-phosphocholine; DPPS, 1,2-dipalmitoyl-*sn*-glycero-3-(phospho-L-serine); MEME, Minimum Essential Medium Eagle; NEAA, nonessential amino acids; FBS, fetal bovine serum; BSA, bovine serum albumin; PBS, phosphate-buffered saline solution; TRITC, tetramethylrhodamine β-isothiocyanate; FITC, fluorescein isothiocyanate; MTT, 3-(4,5-dimethylthiazol-2-yl)-2,5-diphenyltetrazolium bromide; TX-100, Triton X-100; DMSO, dimethyl sulfoxide; DAPI, 4′,6-diaminidino-2-phenylindole.

10.1021/bi0502644 CCC: $30.25
Published on Web 07/07/2005

porcine renal epithelial cells (LLC-PK1) (*12*), and peptides into rat pheochromocytoma cells (PC-12) (*13*). The unspecificity of this peptide is a potential advantage for ubiquitous applications.

It has been shown that pep-1 translocates across lipidic vesicles only when a negative transmembrane potential exists (*14*). However, it is not known if endocytosis is also involved in pep-1 translocation in vivo as described for CPPs Tat 48−60 and $(Arg)_9$ (*5*, *9*). Furthermore, it is necessary to determine if the translocation of cargo proteins via pep-1 follows a mechanism identical to that of the free peptide.

In this work, we used β-galactosidase (β-Gal) from *Escherichia coli* as the cargo protein. β-Gal is a homotetramere with an enzymatic activity (EC 3.2.1.23) that is easy to assess and dependent on its quaternary structure (*15*). Each subunit contains 1023 amino acid residues (116 kDa), with 38 Trp residues that enable a characterization by fluorescence spectroscopy. The formal global charge at pH 7.4 is approximately −38 (the estimated charged is based on the pK_a's for the isolated amino acids and was determined using the software available at www.scripps.edu/~cdputnam/protcalc.html).

In this work, we have studied formation of the pep-1−β-Gal complex and its translocation across membranes. We have found that β-Gal translocation into LUV and human HeLa cells depends on the negative transmembrane potential. Alternative pathways, such as classical and caveolin-mediated endosomal pathways, or possible pore formation induced by pep-1, did not account for translocation of β-Gal into the HeLa cells.

EXPERIMENTAL PROCEDURES

Reagents. Pep-1 (Ac-KETWWETWWTEWSQPKKKRKV-cysteamine) that was >95% pure was obtained from GenScript Corp. (Piscataway, NJ). β-Gal from *E. coli*, 4-methylumbelliferyl galactoside (MUG), porcine pancreatic lyophilized trypsin, phenylmethanesulfonyl fluoride (PMSF), cholesterol (chol), Triton X-100 (TX-100), and dextran (M_r = 10 000) were obtained from Sigma-Aldrich (St. Louis, MO). Tris(2-cyanoethyl)phosphine (phosphine) and dextran tetramethylrhodamine β-isothiocyanate (TRITC) conjugate (M_r = 10 000) were from Molecular Probes (Eugene, OR). 1-Palmitoyl-2-oleoyl-*sn*-glycero-3-phosphocholine (POPC), 1-palmitoyl-2-oleoyl-*sn*-glycero-3-[phospho-*rac*-(1-glycerol)] (POPG), 1,2-dipalmitoyl-*sn*-glycero-3-phosphocholine (DPPC), and 1,2-dipalmitoyl-*sn*-glycero-3-(phospho-L-serine) (DPPS) were from Avanti Polar-Lipids (Alabaster, AL); Minimum essential medium Eagles with Earle's salts (MEME), L-glutamine, nonessential amino acids (NEAA), fetal bovine serum (FBS), streptomycin and penicillin, and trypsin-EDTA solution (0.05% trypsin and 0.53 mM EDTA·4Na) were obtained from Gibco Invitrogen Corp. (Carlsbad, CA). 4′,6-Diaminidino-2-phenylindole (DAPI) was from Sigma. The primary antibodies used were as follows: mouse monoclonal anti-β-Gal (AB1; 1/500 dilution) from Promega (Madison, WI), rabbit polyclonal anti-β-Gal (AB2; 1/500) from 5Prime (Boulder, CO), mouse monoclonal anti-EEA1 (1/100) from BD Biosciences (Palo Alto, CA), mouse monoclonal anti-cathepsin D (1/20) from Sigma-Aldrich (St. Louis, MO), and rabbit polyclonal anti-caveolin-1 (1/50) from Santa Cruz Biotechnology (Santa Cruz, CA). The secondary antibodies were goat polyclonal anti-mouse IgG TRITC conjugate (1/60) and goat polyclonal anti-rabbit IgG fluorescein isothiocyanate (FITC) conjugate (1/100) obtained from Sigma-Aldrich.

Photophysics of β-Gal in Aqueous Solution. The experiments in aqueous solution and with LUV were performed at room temperature with a UV−vis Jasco V-530 spectrophotometer and a SLM Aminco 8100 spectrofluorometer (equipped with a 450 W Xe lamp and double monochromators). The solutions were prepared in 10 mM HEPES buffer (pH 7.4) containing 150 mM NaCl, at physiologic ionic strength. Fluorescence intensities were corrected for the inner filter effect with the equation $I_c = I \times 10^{0.5A}$, where I_c is the corrected intensity, I the measured intensity, and A the absorbance at the excitation wavelength.

Protein photophysical characterization was carried out by means of Trp fluorescence emission ($\lambda_{excitation}$ = 280 nm). Fluorescence emission characterization and determination of quantum yield (*16*) were performed. Variation of fluorescence emission intensity with concentration (0−269 nM) and fluorescence quenching by acrylamide (aqueous soluble Trp quencher) were carried out in the absence and presence of a reducing agent, 1 mM phosphine. The quenching assay was performed by titration of β-Gal with acrylamide (0−60 mM) and followed by fluorescence emission with a $\lambda_{excitation}$ of 290 nm (to minimize the relative quencher/fluorophore light absorption ratio). The Stern−Volmer equation ($I_0/I = 1 + K_{SV}[Q]$, where I and I_0 are the fluorescence intensity in the presence and absence of quencher, respectively, K_{SV} is the Stern−Volmer constant, and [Q] is the concentration of quencher; for a revision, see ref *17*) was applied to the data. Data were corrected for simultaneous absorption of the fluorophore and quencher (see eq *5* in ref *18*).

Enzymatic Assay of β-Gal. Enzyme activity of β-Gal was determined by hydrolysis of 4-methylumbelliferone β-D-galactopyranoside (MUG), a nonfluorescent substrate, to 4-methylumbelliferone (4-MU), a fluorescent product ($\lambda_{excitation}$ = 360 nm, $\lambda_{emission}$ = 440 nm) (*19*). Time progression curves were performed (0−60 min); briefly, enzyme was added to 2.5 mM MUG (substrate at nonlimiting concentrations), in 10 mM HEPES buffer (pH 7.4), containing 150 mM NaCl, to start the reaction. The reaction was stopped by the addition of 0.2 M NaOH-containing buffer (to a final substrate dilution of 1/40, pH 13.2). The assay was followed by 4-MU fluorescence intensity. The concentration was determined by A_{360} [$\epsilon_{360} = 1.9 \times 10^4$ M^{-1} cm^{-1} (*20*)].

Formation of the Pep-1−β-Galactosidase Complex. The titration of 72 nM protein with peptide was performed up to a pep-1/β-Gal molar ratio of 100. Trp fluorescence emission spectra were monitored to follow complex formation. The maximum of the fluorescence emission spectrum of β-Gal occurs at a wavelength significantly different from that of pep-1 (329 nm vs 346 nm). The fluorescence emission spectra of pep-1 in the absence of β-Gal and vice versa were followed simultaneously, under the same conditions. Enzymatic activity of β-Gal and quenching of Trp fluorescence by acrylamide at different pep-1/β-Gal ratios was followed as mentioned above.

Interaction of β-Gal and the Pep-1−β-Gal Complex with Large Unilamellar Vesicles. LUV were prepared, in 10 mM HEPES buffer (pH 7.4) containing 150 mM NaCl, by the

extrusion method (*21*). To evaluate the interaction of 72 nM β-Gal (free or complexed with pep-1 at different concentrations) with LUV, Trp fluorescence spectral shifts were followed ($\lambda_{excitation} = 280$ nm) by titration of samples with lipidic suspensions (0−3.75 mM). POPC and POPC/POPG (4/1) bilayers in vesicles are in liquid crystalline phases; POPC/chol (2/1) bilayers in vesicles are in the liquid-ordered phase, and DPPC and DPPC/DPPS (4/1) bilayers are in the gel phase.

Uptake of the Pep-1−β-Gal Complex in LUV with Negative Transmembrane Potential. The pep-1−β-Gal complex (molar ratio of 320) was incubated (30 min) with POPC/POPG (4/1) (final lipid concentration of 0.5 mM) LUV in the absence or presence of negative transmembrane potential (see ref *14* for a description of production of LUV with a negative transbilayer potential). Briefly, valinomycin was added, at a $1/10^4$ molar ratio (moles per mole of lipid), to K^+-loaded LUV dispersed in Na^+ buffer. Afterward, a trypsin solution (final concentration of 1.3 mM) was added, and the mixture was allowed to digest the nonincorporated pep-1 and β-Gal, incubated for 30 min at 37 °C. After that, incubation with 4 mM PMSF (final concentration) was carried out for 15 min to inhibit trypsin. To induce LUV permeabilization and leakage of the incorporated β-Gal, 0.2% (w/v) TX-100 was added. Released β-Gal was detected by means of its enzymatic activity, namely, by MUG hydrolysis during 20 min at 37 °C followed by fluorescence spectroscopy, as described above. Controls without pep-1 were performed, and the slight contribution from nonincorporated β-Gal resistant to trypsin hydrolysis was discounted.

Cell Culture and Cell Viability Assays. Adherent human negroid cervix epitheloid carcinoma cells (HeLa) were grown in MEME supplemented with 2 mM Glu, 2 mM NEAA, 10% (v/v) FBS, and 1% (v/v) streptomycin and penicillin, in a 5% CO_2 humidified atmosphere at 37 °C. Cells were split in a 1/4 dilution every 3−4 days, after they reached confluency, which was monitored using an inverted microscope (Olympus CK30). Cell viability was determined by the colorimetric assay with 3-(4,5-dimethylthiazol-2-yl)-2,5-diphenyltetrazolium bromide (MTT). MTT is reduced by mitochondrial dehydrogenases of viable cells (*22*). Briefly, cells were grown in 96-well plates and washed with serum-free medium; 10 μL of MTT (5 mg/mL) was added to each well, and a 3 h incubation at 37 °C was performed. The purple product was solubilized in dimethyl sulfoxide (DMSO), and the absorbance at 540 nm was determined. Alternatively, cell viability was determined by the trypan blue exclusion assay. Briefly, after being detached, the cell suspension was added to a trypan blue solution (1/10 dilution) and counted in hemacytometer. Viable cells exclude trypan blue; nonviable cells absorb the dye and appear blue.

Cellular Uptake of Proteins and Dextran Monitored by Immunofluorescence Microscopy. For immunofluorescence microscopy, cells were grown on 12 mm diameter glass coverslips in 24-well plates to approximately 70% confluence. Prior to the uptake assays, the pep-1−β-Gal complex was formed in serum-free medium (*23*) during 30 min at room temperature following the instructions of the supplier (*Active Motif*; Rixensart) (*24*). Translocation efficiency was evaluated with different pep-1/β-Gal ratios (4, 32, 100, 200, 320, 600, and 1000) at 10.8 nM β-Gal. Coverslips were inverted and placed over a drop of a macromolecular complex solution (*25*) and incubated for 60 min at 37 °C. Cells were washed three times in PBS containing 0.5 mM $MgCl_2$, fixed in 4% (w/v) paraformaldehyde for 20 min, permeabilized with 0.1% (w/v) TX-100 for 15 min, and then incubated in a blocking solution that consisted of PBS containing 1% bovine serum albumin (BSA) for 1 h (*26*). After that, incubations with primary and secondary antibodies in blocking solution, for 2 and 1 h, respectively, were performed. Washings were carried out in PBS. Coverslips were mounted in Airvol and observed in the Leica DMRB fluorescence microscope and/or in the Bio-Rad MRC1024 confocal microscope. The nucleus was visualized with DAPI that was added to the secondary antibody mixture at a dilution of 1/1000. The kinetics of the β-Gal translocation process was evaluated by incubation at a pep-1/β-Gal ratio of 320 for 10, 20, 30, 40, 50, 60, and 120 min at 4 or 37 °C. Enzymatic activity of internalized β-Gal by HeLa cells was monitored by the use of MUG (see Enzymatic Assay of β-Gal). After incubation of the complex for 60 min at 4 or 37 °C, trypsin was added to the cells to hydrolyze nonincorporated peptide and protein. Cells were centrifuged at 500*g* for 5 min, washed twice in PBS, and resuspended in 0.1% (w/v) TX-100 for 15 min for permeabilization. Then 2 mM substrate was added to cells, and product progression curves were followed for 120 min at 37 °C. NaOH was added, and product formation was monitored as described above. A control without pep-1 was carried out.

The uptake of the anti-mouse IgG−TRITC conjugate mediated by pep-1 was monitored by immunofluorescence microscopy under live conditions, without the paraformaldehyde fixation step, in a 60 min incubation at 4 or 37 °C, at a 1/320 protein/pep-1 ratio.

Cells were also incubated with the endocytic tracer dextran−TRITC at 2 mg/mL associated with pep-1, at 37 and 4 °C for 60 min, in the presence or absence of 20 mg/mL nonlabeled dextran.

Confocal Microscopy and Colocalization Analysis. For each picture, laser intensities and amplifier gains were adjusted to prevent pixel saturation. This was done using GLOW LUT in the Leica Confocal software. Each fluorophore that was used was excited and detected separately to avoid any signal crossover. Each picture consisted of a z-series of 14 images of 1024 × 1024 pixel resolution with a pinhole Airy unit. Colocalization analysis was performed using open source Image J version 1.30 (http://rsb.info.nih.gov/ij/). The procedure was applied for a population of 6−10 cells. Quantification of colocalization of β-Gal (AB1 or AB2) with endosomes (anti-EEA1), lysosomes (anti-cathepsin D), and caveosomes (anti-caveolin-1) was based on that previously described (*27*).

Effect of Transmembrane Potential on the Uptake of the Pep-1/β-Gal Complex by HeLa Cells. To decrease the transmembrane potential, cells were incubated, for 30 min at 37 °C, with the pep-1−β-Gal complex preformed in PBS buffer, containing different K^+ concentrations, with Na^+ replaced by K^+, at increasing concentrations (*28*). Quantification of internalized β-Gal was carried out by using enzymatic activity. Cell viability in the presence of different K^+ concentrations was determined by the trypan blue exclusion method. Absolute fluorescence intensity data were divided by the number of viable cells.

RESULTS

Formation of the Pep-1−β-Gal Complex in Aqueous Solution. To investigate the suitability of β-Gal for cellular uptake studies mediated by pep-1, characterization of the protein and the complex formed in aqueous solution has been performed. Each subunit of β-Gal contains 38 Trp, 35 Phe, and 25 Tyr residues. Fluorescence emission with a $\lambda_{excitation}$ of 280 nm is largely dominated by the Trp residues. Most hydrophobic residues are not accessible to the aqueous environment as concluded from the β-Gal crystallographic structure. In aqueous solution, fluorescence emission has a quantum yield (Φ) of 0.099 ± 0.005 (constant up to 269 nM) with a band maximum at 329 nm which was significantly different from the maximum of free Trp. This blue-shifted emission is in agreement with most of the Trp residues being inaccessible to the aqueous environment. The low accessibility of Trp residues to the aqueous environment was confirmed by acrylamide quenching; K_{SV} was significantly lower from that obtained for free Trp (5.6 ± 0.3 and 18.9 ± 0.3 M^{-1}, respectively). The initial velocity of MUG hydrolysis, catalyzed by β-Gal, was 17.5 μM min^{-1}, and linearity was maintained for 30 min.

Since the cytoplasm is a reducing environment, we have tested the effect of the reducing agent phosphine (1 mM) on β-Gal conformation and activity. The quantum yield was slightly decreased (Φ = 0.067 ± 0.007), but the accessibility of Trp to aqueous solution (K_{SV} by acrylamide is 5.4 ± 0.2 M^{-1}) was not altered. A concomitant slight decrease in the initial velocity of enzymatic activity occurred (12.0 μM min^{-1}).

The initial velocity of the enzymatic reaction catalyzed by β-Gal was maintained up to a peptide/protein molar ratio of 16. In this range, the peptide strongly interacts with the protein (see the Supporting Information for experimental results and discussion). The initial velocity decreased to 78% (v_0 = 13.4 μM min^{-1}) and 54% (v_0 = 9.4 μM min^{-1}) of the starting value at pep-1/β-Gal ratios of 40 and 400, respectively. In a reducing environment, a more pronounced decrease was observed: for the 400 complex, v_0 = 5.8 μM min^{-1}, which corresponded to a reduction of 52% of the enzymatic activity in the absence of pep-1 (12.0 μM min^{-1}).

Transmembrane Potential Is Required for Translocation of the Pep-1−β-Gal Complex into LUV. No spectral alterations occurred when β-Gal was in the presence of neutral or negatively charged LUV [POPC, POPC/POPG (4/1), POPC/chol (2/1), DPPC, and DPPC/DPPS (4/1)] (Table 1). A slight blue shift in emission spectra was detected for pep-1−β-Gal complexes (molar ratios of 4, 16, 38, 60, and 400) in POPC, POPC/POPG (4/1), and POPC/chol (2/1) lipidic systems (Table 1).

We investigated the uptake of β-Gal mediated by pep-1 into LUV after the induction of an electrostatic gradient across the membrane by valinomycin. Briefly, after a 30 min incubation with the complex, hydrolysis of the pep-1−β-Gal complex outside LUV was achieved with trypsin; then the activity of β-Gal enclosed in the LUV lumen was determined after release with TX-100. Product formation concentration was enhanced by a factor of 5 in the presence of the negative transmembrane potential (when compared with the situation without a potential). The fraction of translocated protein is low, which is expected considering the total volume of the vesicles in the total bulk solution (~0.016%).

Table 1: Partition of the Pep-1−β-Gal Complex into LUV[a]

lipid	sample	aqueous solution (nm)	3.75 mM lipid (nm)	shift (nm)[b]
POPC	β-Gal	329	329	0
	pep-1−β-Gal (4/1)	330	325	5
	pep-1−β-Gal (16/1)	331	327	4
	pep-1−β-Gal (38/1)	336	332	4
	pep-1−β-Gal (60/1)	337	332	5
	pep-1−β-Gal (400/1)	343	336	7
	pep-1	346	338	8
POPC/POPG (4/1)	β-Gal	329	329	0
	pep-1−β-Gal (4/1)	330	327	3
	pep-1−β-Gal (16/1)	332	330	2
	pep-1−β-Gal (38/1)	337	333	4
	pep-1−β-Gal (60/1)	335	331	4
	pep-1	346	338	8
POPC/chol (2/1)	β-Gal	329	329	0
	pep-1−β-Gal (4/1)	330	325	5
	pep-1−β-Gal (16/1)	331	325	3
	pep-1−β-Gal (38/1)	335	330	5
	pep-1−β-Gal (60/1)	341	336	5
	pep-1	346	337	9

[a] Maximum fluorescence emission of the pep-1−β-Gal complex, at different ratios, in aqueous solution [10 mM HEPES buffer containing 150 mM NaCl (pH 7.4)] and in the presence of a 3.75 mM lipidic suspension. [b] The shift is the difference between the two conditions.

Therefore, these results indicate not only that pep-1 improves the affinity of the protein for the membrane but also that the presence of a transmembrane potential induces its translocation across a bilayer.

Pep-1 Does Not Induce Pore Formation in HeLa Cells. It has been suggested that protein uptake mediated by pep-1 involves pore formation (*29*), but this is controversial in light of biophysical studies with lipidic vesicles (*14*). To test this hypothesis, we have determined the cell viability by the trypan blue exclusion method. This method relies on the inclusion of the dye trypan blue by dead cells once their plasma membrane is permeable or damaged. If pep-1 would induce pores on the plasma membrane of cells, a larger amount of intracellular trypan blue would be observed. However, this was not the case since viabilities were similar for control cells (96.4 ± 0.6%) or cells incubated with pep-1 and the pep-1−β-Gal complex (95.5 ± 1.6 and 95.6 ± 0.1%, respectively). These results indicated that pep-1 did not induce permeability changes and hence pore formation in the plasma membrane of HeLa cells.

To evaluate the possible toxic effect of pep-1 on the cells, we have used an independent cell viability test, the MTT assay. MTT is a very sensitive way of determining cytotoxicity. In living cells, mitochondrial dehydrogenase enzymes oxidize the yellow MTT and convert it into purple formazan crystals (*22*). It was observed that the peptide induced a reduction in cell viability of approximately 22%. Since viability calculated by the trypan blue assay was not decreased after addition of pep-1, these results suggested that pep-1 might inhibit mitochondrial dehydrogenases.

Electrostatic Transmembrane Potential Is a Sine-Quanon Requirement for Translocation of the Pep-1−β-Gal Complex into HeLa cells. To monitor the uptake of the pep-1−β-Gal complex by HeLa cells, increasing pep-1 concentrations and

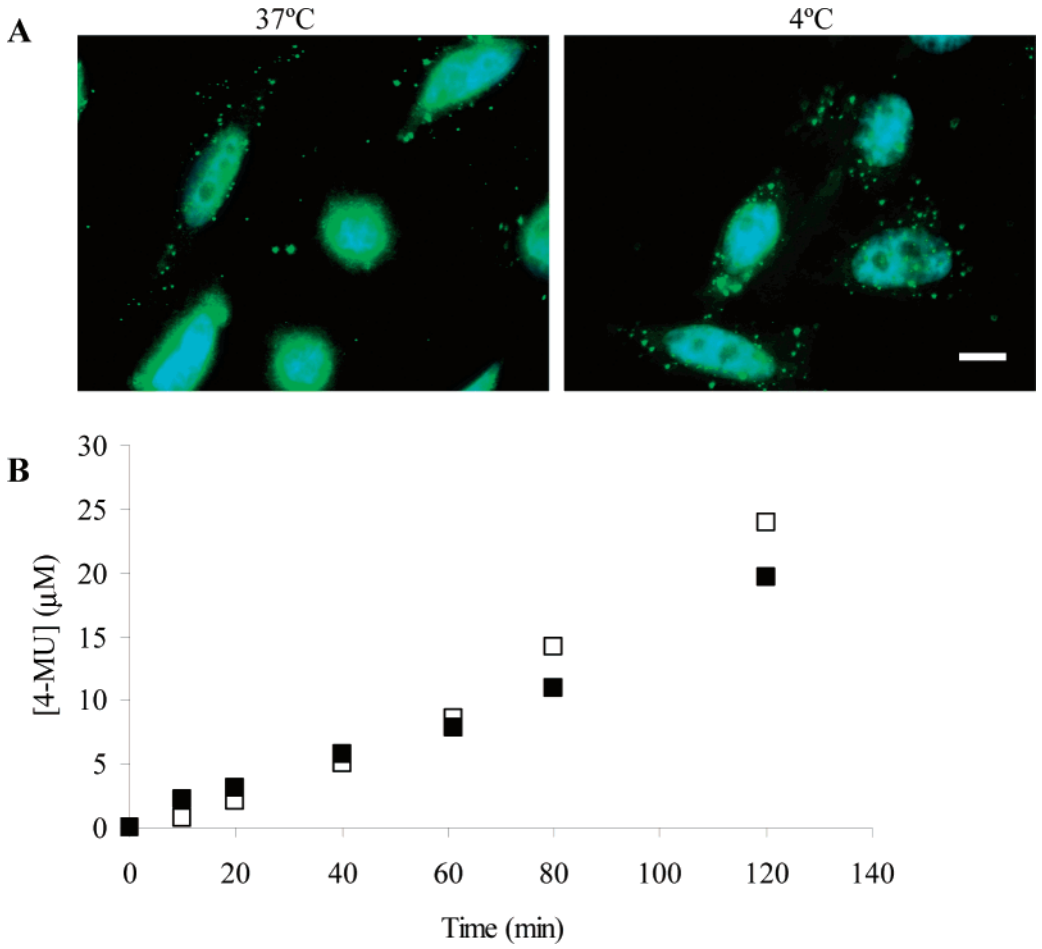

FIGURE 1: Translocation of β-Gal, mediated by pep-1, into HeLa cells. Panel A shows immunofluorescence microscopy detection of β-Gal. The pep-1−β-Gal complex (molar ratio of 320) was incubated with HeLa cells, at 37 or 4 °C, for 60 min. Cells were fixed with 4% paraformaldehyde and permeabilized with 0.1% (w/v) TX-100. β-Gal was detected with rabbit polyclonal anti-β-Gal and the secondary anti-rabbit antibody coupled to FITC. DAPI was used to identify the nucleus. Internalized β-Gal is in the cytosol. The scale bar is 10 μm. Panel B shows enzymatic activity of β-Gal internalized in a HeLa cell suspension. β-Gal uptake, after incubation with the pep-1−β-Gal complex (molar ratio of 320) for 60 min at 4 (■) or 37 °C (□), was followed by the progression curve of enzymatic MUG hydrolysis, at 37 °C. The control without pep-1 was subtracted. The formation of 4-MU monitored by fluorescence intensity at 440 nm with excitation at 360 nm indicates that β-Gal was efficiently translocated, at both temperatures, in an active form.

different incubation times have been tested. After a 60 min incubation at a pep-1/β-Gal ratio of 320, a significant uptake of β-Gal has been observed (Figure 1A). β-Gal was found dispersed in aggregates within the cytosol. The presence of protein inside the cell and not adsorbed on the cell surface was confirmed by confocal microscopy. Apparently, the translocation efficiency did not increase for complex ratios between 320 and 1000. For lower ratios, between 4 and 200, uptake of β-Gal did not occur. Therefore, the chosen pep-1/β-Gal ratio for all the experiments was 320. At this ratio, there was an excess of soluble pep-1 in solution (see Figure S1 of the Supporting Information).

Transfection was relatively fast; after 10 min, it was already possible to identify a small quantity of protein in some cells. The level of transfection increased until approximately 40 min; after this time, it seemed to stabilize (data not shown). Translocation occurred with a similar efficiency at 4 °C (Figure 1A). To test if β-Gal was active after translocation, MUG hydrolysis was monitored in cells incubated at 37 and 4 °C with the complex. It was observed that β-Gal was indeed active after translocation at both temperatures (Figure 1B).

For a typical animal cell characterized by dominant potassium permeability, increasing the external potassium concentration necessarily reduces the transmembrane potential due to the decrease in the electrochemical gradient of K^+ across the cell membrane (*28*, *30*). Negative transmembrane potential is dominated by potassium potential equilibrium, which can be estimated by the potassium Nernst potential (E_K): $E_K = (RT/F) \ln(K_0/K_i)$, where R is the gas constant, T is the absolute temperature, F is Faraday's constant, and K_0 and K_i are the extracellular and intracellular potassium concentrations, respectively. So, increasing the extracellular K^+ concentration leads to less negative Nernst potentials (Figure 2).

To test if the electrostatic membrane potential would be required for translocation of the pep-1−β-Gal complex, HeLa cells have been incubated with the complex at increasing external K^+ concentrations. The total ionic strength ($[K^+] + [Na^+] = 150$ mM) was kept constant. The internalized β-Gal concentration was estimated from enzymatic MUG hydrolysis. This assay was performed for 30 min to guarantee that the initial velocity of the reaction was maintained, and that the concentration of β-Gal uptake was directly related

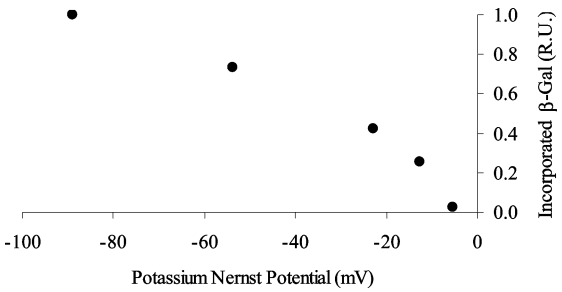

FIGURE 2: Variation of uptake of β-Gal into a HeLa cell suspension, mediated by pep-1, with potassium Nernst potential. The pep-1−β-Gal complex (molar ratio of 320) was incubated with HeLa cells, for 30 min at 37 °C, in the presence of increasing external K^+ concentrations, and a constant ionic strength ($[K^+] + [Na^+] = 150$ mM). The relative level of β-Gal uptake was determined from β-Gal enzymatic hydrolysis of MUG for 20 min at 37 °C. The potassium Nernst potential was determined considering an internal K^+ concentration of 140 mM; the external K^+ concentration ranged from 5 to 114.6 mM, which corresponded to a range from −89 to −5.4 mV, respectively (see the equation in the text). An increasing external K^+ concentration severely reduces the level of β-Gal uptake.

with 4-MU production. A decrease in the absolute value of the electrochemical K^+ gradient (calculated considering K_i = 140 mM) led to a severe drop in the level of β-Gal uptake (Figure 2). When K_0 = 114.6 mM, uptake was almost completely inhibited.

Although for low extracellular K^+ concentrations the contribution of other conductors makes the membrane potential less negative than that predicted by K^+ Nernst potential (*28*), the dependence of β-Gal uptake on transmembrane K^+ Nernst potential was clear.

The Pep-1−β-Gal Complex Is Not Internalized by HeLa Cells via the Endosomal Pathways. Other CPPs such as the one derived from TAT and $(Arg)_9$ (*5*) seem to translocate proteins across cells by two different mechanisms: one is fast and physical in nature and the other is mediated by endocytosis. In the case of an endosomal-dependent pathway of β-Gal uptake mediated by pep-1, colocalization with endosomes or lysosomes at some extension would be expected. To evaluate this possibility, colocalization of pep-1-translocated β-Gal with EEA1 (early endosomal marker), caveolin-1 (caveosomes marker), and cathepsin D (lysosomal marker) was performed. Monitoring localization of the protein, instead of a fluorescence-labeled pep-1, is a better choice. It prevents problems associated with the apparent uptake of cationic peptides bound to negatively charged membranes, causing an artifactual localization in cells (*5*) and the possible influence of the fluorescent label in the uptake and intracellular localization of the peptide (*31*). The percentages of colocalization with each of the organelles from the endocytic pathway determined after immunofluorescence confocal microscopy were very low (shown on the right in Figure 3), after incubation for 60 or 120 min. Similar results were obtained at 4 °C. These results indicate that the uptake of β-Gal did not involve the endocytic pathway.

It has been suggested that fixation conditions could lead to an artifactual uptake of cationic peptides associated with the cell membrane at 4 °C (*5*, *9*, *32*). The uptake of a protein

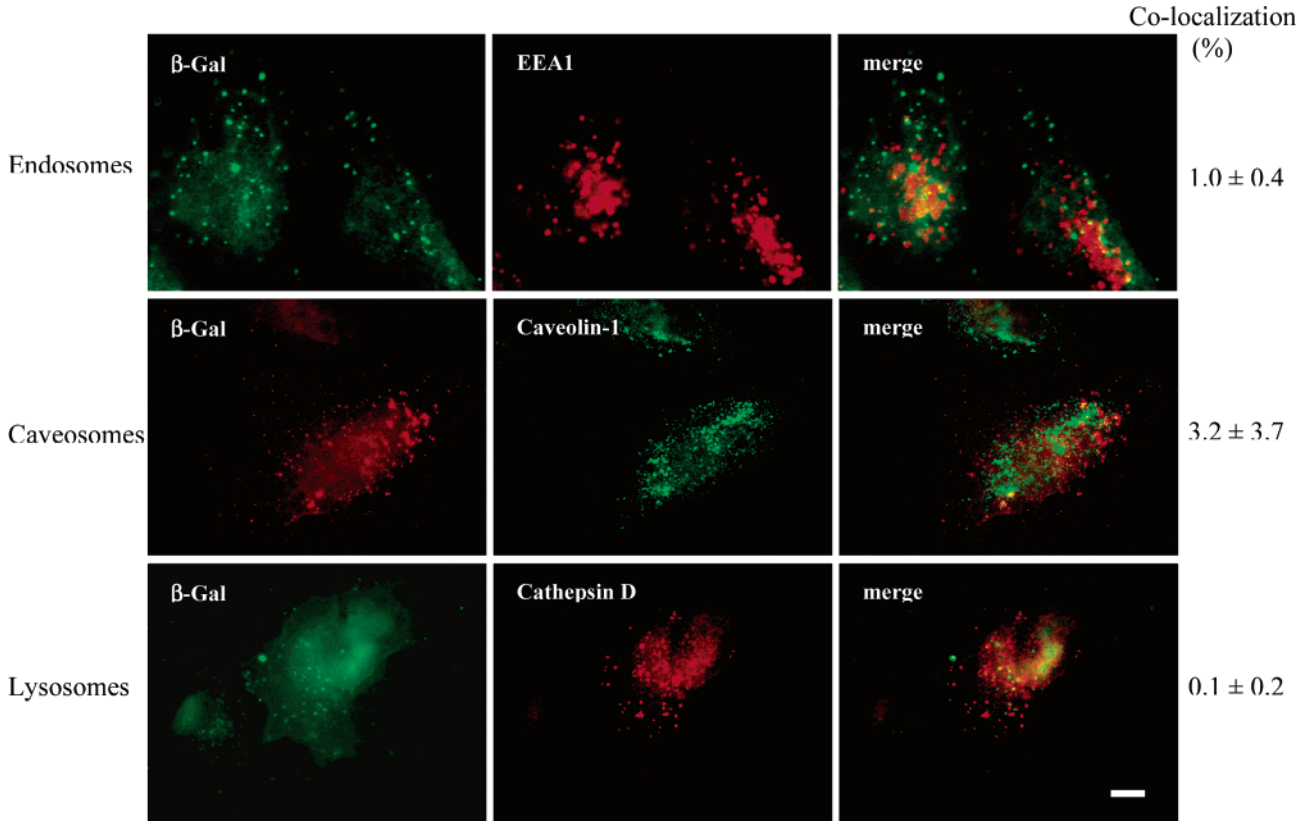

FIGURE 3: Immunofluorescence microscopy localization of pep-1-translocated β-Gal, EEA1, caveolin-1, and cathepsin D from HeLa cells. Cells were incubated with the pep-1−β-Gal complex (molar ratio of 320) for 60 min. Cells were fixed with 4% paraformaldehyde and permeabilized with 0.1% (w/v) TX-100. β-Gal, detected with rabbit polyclonal or mouse monoclonal antibodies, was colocalized with early endosomal EEA1, caviosomal caveolin-1, and lysosomal cathepsin D. Secondary antibodies were the anti-rabbit antibody coupled to FITC and the anti-mouse antibody coupled to TRITC. Pictures of a *z*-series of 14 images from the confocal microscope were analyzed with Image J version 1.3 to perform colocalization analysis. Six to 10 cells were observed. The scale bar is 10 μm.

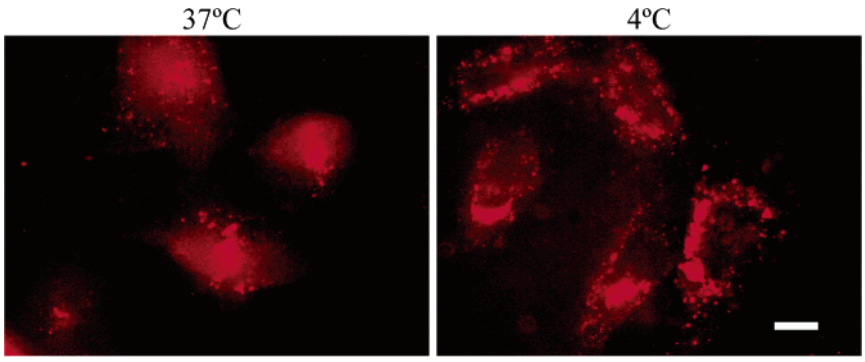

FIGURE 4: Uptake into HeLa cells of anti-mouse antibody conjugated with TRITC, mediated by pep-1. Incubation of cells with a pep-1−anti-mouse−TRITC complex was performed for 60 min at 4 or 37 °C. Cells were visualized under live conditions in a fluorescence microscope. The scale bar is 10 μm.

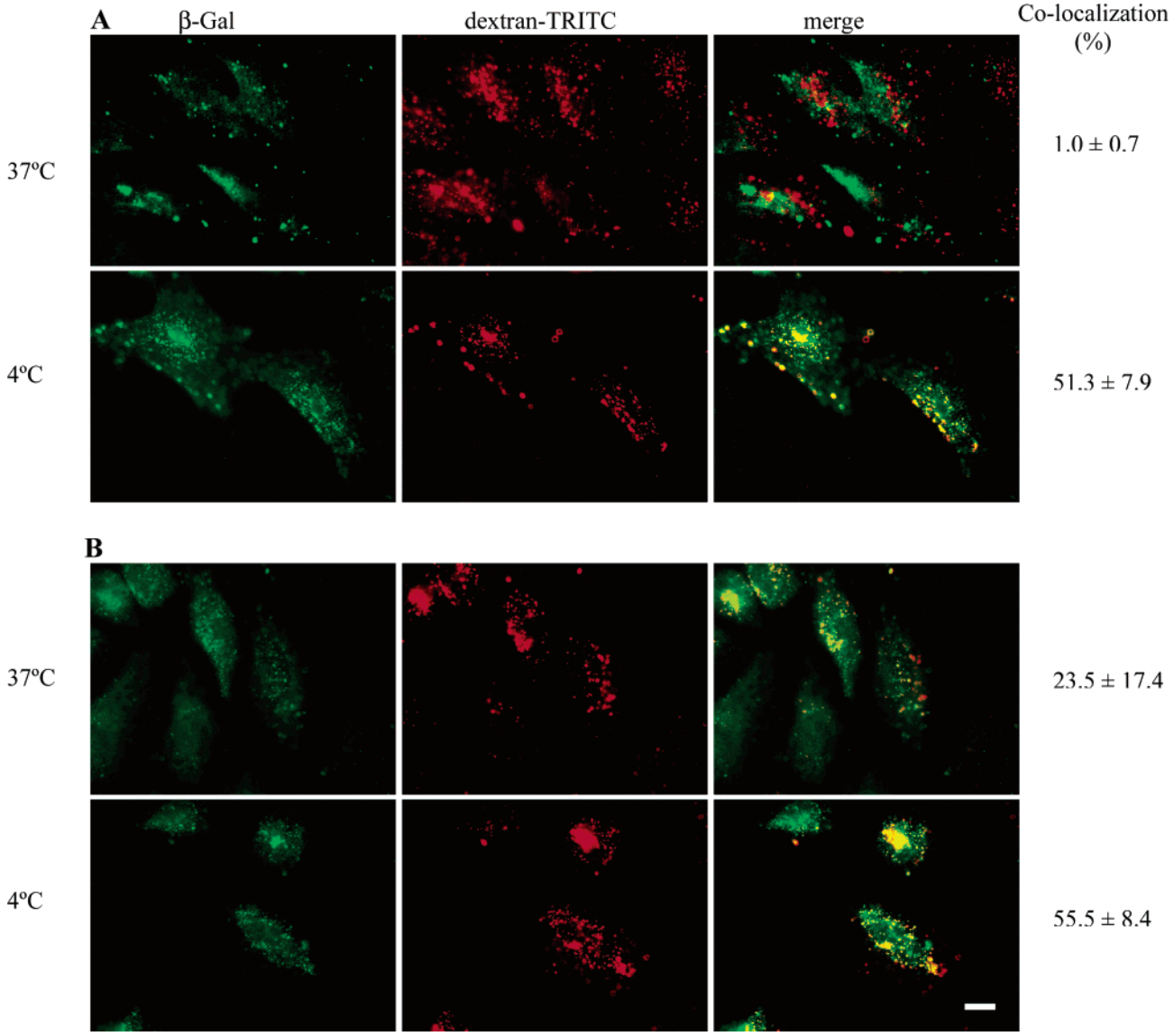

FIGURE 5: Immunofluorescence microscopy localization of translocated β-Gal and the dextran−TRITC marker in HeLa cells (incubation for 60 min at 37 or 4 °C). Panel A shows incubation with the pep-1−β-Gal complex (molar ratio of 320) where the endocytic dextran−TRITC marker (2 mg/mL) was added to the complex at the time of cell incubation. Panel B shows incubation with the preformed pep-1−β-Gal−dextran−TRITC complex. Cells were fixed with 4% paraformaldehyde and permeabilized with 0.1% (w/v) TX-100. β-Gal was detected with rabbit polyclonal anti-β-Gal and anti-rabbit antibodies coupled to FITC. Pictures of a *z*-series of 14 images from the confocal microscope were analyzed with Image J version 1.3 and were used to perform colocalization analysis. Six to 10 cells were used. The scale bar is 10 μm.

covalently marked with a fluorescent probe can be visualized by fluorescence microscopy without the need to fixate or permeabilize the cells. The uptake of anti-mouse TRITC at 4 and 37 °C was performed and visualized by immunofluorescence microscopy without fixation (Figure 4). It was possible to identify the presence of protein inside the cell at

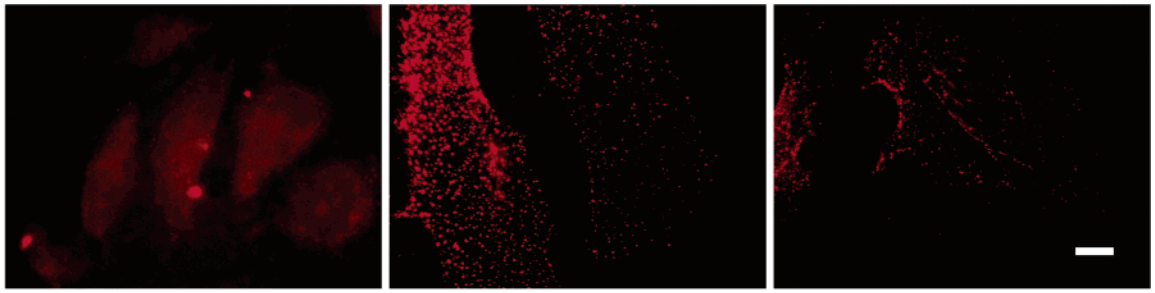

pep-1	-	+	+
dextran-TRITC (2mg/mL)	+	+	+
dextran (20mg/mL)	-	-	+

FIGURE 6: Uptake of the dextran−TRITC marker, mediated by pep-1, into HeLa cells. Comparison of dextran−TRITC (2 mg/mL) uptake, mediated by pep-1, at 4 °C for 60 min when the dextran−TRITC−pep-1 complex was preformed in the presence or absence of dextran (20 mg/mL). Cells were fixed with 4% paraformaldehyde and permeabilized with 0.1% (w/v) TX-100. The dextran−TRITC marker at 4 °C was detected only when pep-1 was present. In the presence of dextran (nonconjugated), the rate of uptake of the dextran−TRITC marker is decreased, indicating a competition of pep-1 for nonconjugated dextran. The scale bar is 10 μm.

both temperatures. This indicated that internalized protein was not an artifact associated with fixation.

The Polysaccharide Dextran Is Translocated into HeLa Cells by Pep-1. Uptake of the dextran−TRITC complex by HeLa cells occurs by a classical endosomal pathway. At 37 °C, β-Gal did not colocalize with the dextran−TRITC marker (1.0%) (Figure 5A), supporting the idea that β-Gal would be translocated into the cells by a mechanism independent of the endocytic pathway. However, at 4 °C, there was an extensive colocalization between β-Gal and the dextran−TRITC marker (51.3%) (Figure 5A). At 4 °C, the classical endosomal pathway is inhibited, so the endocytic dextran−TRITC marker did not enter the cells via this pathway (see control in Figure 6, left image). The internalization of the dextran−TRITC marker at 4 °C and its colocalization with β-Gal suggested that the uptake of translocation of the polysaccharide was mediated by pep-1. However, if the dextran−TRITC marker was preincubated together with pep-1 and β-Gal, a ternary complex seems to be formed and β-Gal−dextran−TRITC colocalization occurred, even at 37 °C (Figure 5B).

To confirm that pep-1 was translocating the dextran−TRITC marker via the polysaccharide without interference of artifacts from the fluorophore moiety, the HeLa cells were incubated with pep-1−dextran−TRITC complex, at 4 °C, in the presence of nonlabeled dextran (Figure 6). It was observed that the presence of nonlabeled dextran dramatically reduced the amount of dextran−TRITC marker translocated into the cells, showing competition between nonlabeled dextran and the dextran−TRITC marker. This confirmed that pep-1 mediated the transport of the polysaccharide into HeLa cells without any artifactual interference of TRITC.

DISCUSSION

β-Gal from *E. coli* was chosen for the study of the interaction of pep-1 with a protein and evaluation of the translocation efficiency inside human tumoral cells. Its enzymatic activity is easy to access. Trp residues enable fluorescence spectroscopy techniques to be used as analytical tools. The absence of a signal sequence makes the protein unable to address any specific organelle inside the cell; therefore, this molecule is very useful in evaluating if the pep-1-mediated translocation leads protein to a specific organelle in human cells. HeLa cells are derived from a human cervix epitheloid carcinoma; they are relatively large (approximately 20 μm) and particularly suitable for organelle visualization by immunofluorescence studies. Therefore, they were chosen as the cellular model system.

β-Gal characterization in aqueous solution and in the presence of LUV revealed that Trp residues are protected from interaction with aqueous solution and no significant interaction with membranes was observed. Enzymatic assays revealed that β-Gal maintains its quaternary structure, which is required for enzymatic activity (*15*) in aqueous solution, under reducing and nonreducing conditions. These results showed that the reducing environment did not modify the β-Gal conformation, so maintenance of enzyme activity inside the cell was expected.

Fluorescence quenching upon the titration of the protein with pep-1 suggests the existence of an excess of pep-1 in solution not interacting with the protein above peptide/protein molar ratios of 60 (data and detailed discussion in the Supporting Information). Enzymatic activity is still detected in the pep-1−β-Gal complex (a molar ratio of up to 400), which eliminates the severe perturbation of β-Gal structure due to pep-1.

The wavelength of maximal fluorescence emission intensity of pep-1 in lipidic membranes systems is higher than that observed for the complex (see Table 1). The blue shift observed for pep-1−β-Gal complexes relative to that of pep-1 alone together with its dependence on the peptide/protein molar ratio showed that pep-1 is mediating the partitioning of β-Gal into lipidic membranes.

Pep-1 translocation in LUV was previously found to be dependent on the transmembrane potential across bilayers (*14*). In fact, in this work, the same was concluded for the translocation of β-Gal mediated by pep-1 in LUV. These results suggested a common translocation mechanism for free and complexed pep-1. This property has been shown previously for other free peptides (*28*, *33*) but is here presented for the first time for a CPP−cargo protein complex, to the best of our knowledge.

β-Gal from *E. coli* was efficiently transported by pep-1 into HeLa cells, maintaining its enzymatic activity. The translocation of protein is dependent on peptide concentration; at a pep-1/β-Gal molar ratio of up to 200, translocation was not detected. With a pep-1/β-Gal ratio of 320, the process is very efficient. At this ratio, there is free pep-1 in solution (see Figure S1 of the Supporting Information), which seems to play a role in the translocation process. An excess of pep-1 is probably necessary for membrane destabilization (*14*), facilitating the uptake of the protein. If the translocation was mediated by pore formation, a very large pore (≈104 Å × 140 Å, estimated from the β-Gal crystallographic structure) would be necessary for a protein as large as β-Gal (116 kDa) to pass across the bilayer. A pore with such a diameter would probably induce leakage of the cellular contents at some extension, compromising cellular viability. Cell viability was maintained in the presence of pep-1 and the complex, and pore formation was not detected. This is in agreement with the study of interaction of pep-1 with LUV (see ref *14*), where pep-1 translocation occurred without pore formation.

The high velocity of the translocation mechanism (10 min was enough to detect protein inside the cell) and the independence of temperature (see Figure 1A,B) suggested a physical mechanism not dependent on complex cellular biochemical processes. This hypothesis was confirmed by the correlation found between cell depolarization and β-Gal translocation. Destroying the potassium electrochemical gradient drastically reduced the level of β-Gal uptake in HeLa cells (see Figure 2). These results are in agreement with those obtained with LUV. Therefore, in vivo the membrane charge asymmetry (*34*, *35*) and the combined effect of membrane potentials (*36*) seemed to be the driving forces responsible for the translocation process.

Inside the cell, the protein was found in the cytosol and did not colocalize with endosomes, lysosomes, or caveosomes (see Figure 3). These results were consistent with a translocation process independent of the classical endosomal pathways or caveolin-mediated endosomal pathways. In the case of endocytosis being a secondary mechanism for uptake, at least a small colocalization with one of these organelles would be expected. Monitoring localization of the protein, instead of pep-1, prevents problems associated with the apparent uptake of cationic peptides bound to negatively charged membranes, causing an artifactual localization in cells (*5*). Lebleu and co-workers found that TAT and oligoarginine uptake was dependent on endocytosis (*5*), but Nordén and co-workers (*9*) have proven that for arginine-rich peptides both nonendocytic and endocytic uptake pathways were involved in their cellular internalization. This nonendocytic mechanism was fast and biologically relevant (*9*). An endocytic pathway was not detected for pep-1, but a physical transmembrane crossing mechanism was.

A translocation mechanism independent of endocytosis was further confirmed under nonfixation conditions with anti-mouse TRITC where protein uptake at 4 °C has been observed (see Figure 4).

The transport of the dextran−TRITC marker mediated by pep-1 under conditions where the endocytosis was inhibited was also demonstrated (see Figures 5 and 6). It has been suggested by Morris et al. (*10*) that pep-1 interacts with macromolecules via hydrophobic interactions. Given the hydrophilic nature of the molecule, the capacity of pep-1 to translocate dextran demonstrated that hydrophobic pockets are not essential for complex formation and uptake. Complex formation of pep-1 and dextran is probably due to polar interactions and hydrogen bonding.

In conclusion, the interaction of pep-1 with β-Gal from *E. coli* was extensively studied to gain insight into the translocation mechanism at the molecular level. It has been demonstrated that pep-1 can establish a variety of electrostatic and/or hydrophobic and/or hydrophilic interactions with the cargo. The existence of a negative transmembrane potential promotes uptake of β-Gal, mediated by pep-1, in vitro and in vivo, and the absence of a transmembrane potential inhibits it. The charge asymmetry (negative inside) seems to be the driving force for translocation to occur. There was no evidence found for the involvement of the endocytic pathway in the uptake of cargo mediated by pep-1. Furthermore, pep-1 did not induce the formation of pores in the membrane. These results together suggested that the peptide and the cargo translocate only by a physical process.

ACKNOWLEDGMENT

We thank Dr. Adriano Henriques (Instituto de Tecnologia Química e Biológica) for the anti-β-galactosidase antibodies. We thank the Cell Imaging Service (IGC, Oeiras, Portugal) for the use of the confocal microscope.

SUPPORTING INFORMATION AVAILABLE

Further experimental results and discussion. This material is available free of charge via the Internet at http://pubs.acs.org.

REFERENCES

1. Wadia, J. S., Becker-Hapak, M., and Dowdy, S. F. (2002) Interactions of cell-penetrating peptides with membranes, in *Cell-penetrating peptides, processes and applications* (Langel, Ü., Ed.) pp 365−375, CRC Press Pharmacology and Toxicology Series, CRC Press, New York.
2. Bogoyevitch, M. A., Kendrick, T. S., Dominic, C. H., and Barr, R. K. (2002) Taking the cell by stealth or storm? Protein transduction domain (PTDs) as versatile vectors for delivey, *DNA Cell Biol. 21*, 879−894.
3. Bonetta, P. (2002) Getting protein into cells, *Scientist 17*, 38−40.
4. Eguchi, A., Akuta, T., Okuyama, H., Senda, T., Yokoi, H., Inokuchi, H., Fujita, S., Hayakama, T., Takeda, K., Hasegawa, M., and Nakanisshi, M. (2001) Protein transduction domain of HIV-1 Tat protein promotes efficient delivery of DNA into mammalian cells, *J. Biol. Chem. 247*, 27205−27210.

5. Richard, J. P., Melikov, K., Vives, E., Ramos, C., Verbeure, B., Gait, M. J., Chernomordik, L. V., and Lebleu, B. (2003) Cell-penetrating peptides, a reevaluation of the mechanism of cellular uptake, *J. Biol. Chem. 278*, 585−590.
6. Schwarze, S. R., Hruska, K. A., and Dowdy, S. F. (2000) Protein transduction: Unrestricted delivery into all cells? *Trends Cell Biol. 10*, 290−295.
7. Chaloin, L., Mau, N. V., Divita, G., and Heitz, F. (2002) Interactions of cell-penetrating peptides with membranes, in *Cell-penetrating peptides, processes and applications* (Langel, Ü., Ed.) pp 23−51, CRC Press Pharmacology and Toxicology Series, CRC Press, New York.
8. Joliot, A., and Prochiantz, A. (2004) Transduction peptides: From technology to physiology, *Nat. Cell Biol. 6*, 189−196.
9. Thorén, P. E. G., Persson, D., Isakson, P., Goksör, M., Önfelt, A., and Nordén, B. (2003) Uptake of analogs of penetratin, Tat(48−60) and oligoarginine in live cells, *Biochem. Biophys. Res. Commun. 307*, 100−107.
10. Morris, M. C., Depollier, J., Mery, J., Heitz, F., and Divita, G. (2001) A peptide carrier for the delivery of biologically active proteins into mammalian cells, *Nat. Biotechnol. 19*, 1143−1147.
11. Wu, Y., Wood, M. D., and Katagiri, F. (2003) Direct delivery of bacterial avirulance proteins intro resistant *Arabidopsis* protoplasts lead to hypersensitive cell death, *Plant J. 33*, 131−137.
12. Ikari, A., Nakaro, M., Kawano, K., and Suketa, Y. (2002) Up-regulation of sodium-dependent glucose transporter by interaction with heat shock protein 70, *J. Biol. Chem. 277*, 33338−33343.
13. Zhou, J., and Hsieh, J.-T. (2001) The inhibitory role of DOC-2/DAB2 in growth factor receptor-mediated signal cascade, *J. Biol. Chem. 276*, 27793−27798.
14. Henriques, S. T., and Castanho, M. A. R. B. (2004) Consequences of nonlytic membrane perturbation to the translocation of the cell penetrating peptide pep-1 in lipidic vesicles, *Biochemistry 43*, 9716−9724.
15. Nichtl, A., Buchner, J., Jaenicke, R., Rudolph, R., and Scheibel, T. (1998) Folding and association of β-galactosidase, *J. Mol. Biol. 282*, 1083−1091.
16. Fery-Forgues, S., and Lavabre, D. (1999) Are fluorescence quantum yields so tricky to measure? A demonstration using familiar stationery products, *J. Chem. Educ. 76*, 1260−1264.
17. Lakowics, J. R. (1999**)** *Principles of fluorescence spectroscopy*, 2nd ed., Kluwer Academic/Plenum, New York.
18. Coutinho, A., and Prieto, M. (1993) Ribonuclease T1 and alcohol dehydrogenase fluorescence quenching by acrylamide. A laboratory experiment for undergraduate students, *J. Chem. Educ. 70*, 425−428.
19. McGuire, J. B. J., James, T. J., Imber, C. J., St. Peter, S. D., Friend, P. J., and Taylor, R. P. (2002) Optimisation of an enzymatic method for β-galactosidase, *Clin. Chim. Acta 326*, 123−129.
20. Haugland, R. P. (2002) *Handbook of fluorescent probes and research products*, 9th ed., Molecular Probes, Eugene, OR.
21. Mayer, L. D., Hope, M. J., and Cullis, P. R. (1986)Vesicles of variable sizes produced by a rapid extrusion method, *Biochim. Biophys. Acta 858*, 161−168.
22. Mosmann, T. (1983) Rapid colorimetric assay for cellular growth and survival: Application to proliferation and citotoxicity assays, *J. Immunol. Methods 65*, 55−63.
23. Coulpier, M., Anders, J., and Ibáñez, C. F. (2002) Coordinated activation of autophosphorylation sites in the RET receptor tyrosine kinase. Importance of tyrosine 1062 for GDNF mediated neuronal differentiation and survival, *J. Biol. Chem. 277*, 1991−1999.
24. Chariot, simple efficient protein delivery system. http://www.activemotif.com/products/cell/chariot.php (accessed May 2005).
25. Tisdale, E. J. (2002) Glyceraldehyde-3-phosphate dehydrogenase is phosphorylated by pyotein kinase C and plays a role in microtubule dynamics in the early secretory pathway, *J. Biol. Chem. 277*, 3334−3341.
26. Sousa, V. L., Brito, C., Costa, T., Lanoix, J., Nilsson, T., and Costa, J. (2003) Importance of Cys, Gln, and Tyr from the transmembrane domain of Human β3/4 fucosyltransferase III for its localization and sorting in the Golgi of baby hamster kidney cells, *J. Biol. Chem. 278*, 7624−7629.
27. Sousa, V. L., Brito, C., and Costa, J. (2004) Delection of the cytoplasmic domain of human α3/4 fucosyltransferase III causes the shift of the enzyme to early golgi compartments, *Biochim. Biophys. Acta 1675*, 95−104.
28. Rothbard, J. B., Jessop, T. C., Lewis, R. S., Murray, B. A., and Wender, P. A. (2004) Role of membrane potential and hydrogen bonding in the mechanism of translocation of guanidium-rich peptides into cells, *J. Am. Chem. Soc. 126*, 9506−9507.
29. Deshayes, S., Heitz, A., Morris, M. C., Charnet, P., Divita, G., and Heitz, F. (2004) Insight into the mechanism of internalization of the cell-penetrating carrier peptide pep-1 through conformational analysis, *Biochemistry 43*, 1449−1457.
30. Chifflet, S., Hernández, J. A., Grasso, S., and Cirillo, A. (2003) Nonspecific depolarization of the plasma membrane potential induces cytoskeletal modifications of bovine corneal endothelial cells in culture, *Exp. Cell Res. 282*, 1−13.
31. Szeto, H. H., Schiller, P. W., Zhao, K., and Luo, G. (2005) Fluorescent dyes alter intracellular targeting and function of cell-penetrating tetrapeptides, *FASEB J.* (in press).
32. Lundberg, M., and Johansson, M. (2002) Positively charged DNA-binding proteins cause apparent cell membrane translocation, *Biochem. Biophys. Res. Commun. 291*, 367−371.
33. Terrone, D., Sang, S. L. W., Roudaia, L., and Silvius, J. R. (2003) Penetratin and related cell-penetrating cationic peptides can translocate across lipid bilayers in the presence of a transbilayer potential, *Biochemistry 42*, 13787−13799.
34. Gennis, R. B. (1989) *Molecular structure and functions*, Springer-Verlag, New York.
35. Manno, S., Takakuwa, Y., and Mohandas, N. (2002) Identification of a functional role for lipid asymmetry in biological membranes: Phosphatidylserine-skeletal protein interactions modulate membrane stability, *Proc. Natl. Acad. Sci. U.S.A. 99*, 1943−1948.
36. O'Shea, P. (2003) Intermolecular interactions with/within cell membranes and the trinity of membrane potentials: Kinetics and imaging, *Biochem. Soc. Trans. 31*, 990−996.

BI0502644